A Kinetic Model of Quantitative Real-Time Polymerase Chain Reaction

Sarika Mehra, Wei-Shou Hu

Department of Chemical Engineering and Materials Science, University of Minnesota, 421 Washington Avenue SE, Minneapolis, MN 55455-0132; telephone: (612) 626-7630; fax: (612) 626-7246; e-mail: acre@cems.umn.edu

Received 19 October 2004; accepted 6 April 2005

DOI: 10.1002/bit.20555

Abstract: Real-time polymerase chain reaction (PCR) is one of the most sensitive and accurate methods for quantifying transcript levels especially for those expressed at low abundance. The selective amplification of target DNA over multiple cycles allows its initial concentration to be determined. The amplification rate is a complex interplay of the operating conditions, initial reactant concentrations, and reaction rate constants. Experimentally, the compounded effect of all factors is quantified in terms of an effective efficiency, which is estimated by curve fitting to the amplification data. We present a comprehensive model of PCR to study the effect of various reactant concentrations on the amplification efficiency. The model is used to calculate the kinetic progression of the target DNA concentration with cycle number under conditions when different species are stoichiometrically or kinetically limiting. The reaction efficiency remains constant for the initial cycles. As the primer concentration becomes limiting, the efficiency is marked by a gradual decrease. This is in contrast to a steep decline under nucleotide limiting conditions. Under some conditions, commonly used experimentally, increasing primer concentration has the adverse effect of reducing the final amplified template concentration. This phenomenon seen at times experimentally is explained by the simulation results under rate limiting enzyme concentrations. Primer dimer formation is shown to significantly affect the reaction rates, effective efficiency, and the estimated initial concentrations. This model, by describing the interplay of the many operating variables, will be a useful tool in designing PCR conditions and evaluating its results.

Keywords: real-time polymerase chain reaction; mathematical model; reaction efficiency

INTRODUCTION

Polymerase chain reaction (PCR) is an elegant technique capable of specifically amplifying a single DNA molecule into billions of copies. This technique is widely used for the analysis of genetic information because it requires a very little amount of nucleic acid sample. Application areas span across the spectrum from genomics and developmental biology to medical diagnostics and neurosciences. With the development of various fluorometric assays, it is possible to monitor the DNA amplification in real-time and quantify the amounts of starting material. Real-time PCR is an extremely sensitive method for the detection of low abundance mRNAs. The mRNA is converted to cDNA using the reverse transcriptase enzyme prior to amplification. The method is also used to determine the degree of amplification and deletion of genes in tumor tissues, analyze cytokine profiles of immune cells, and detect mRNA splice variants (Bustin, 2000; Giulietti et al., 2001; Jung et al., 2000). There are several variations of the real-time PCR technique. In quantitative competitive RT-PCR, a ''competitor'' is coamplified with the target sample in the same reaction. Same set of primers is used to amplify both the target and the slightly modified competitor. In Multiplex RT-PCR, multiple primer sets are used to simultaneously amplify several targets from the same sample.

A fluorescent DNA binding dye is used to detect the amplification of the target DNA at each cycle. The initial concentration can therefore be estimated by calculating the number of cycles that are required to attain a chosen threshold concentration of the target DNA. The cycle at which this threshold concentration, $D_{\text{threshold}}$, is achieved is called the C_T value. Various detection systems, including the Taqman® and SYBR Green, are available for this purpose (Bustin, 2000). The Taqman® system uses a fluorescent resonance energy transfer (FRET) probe as a reporter system along with the forward and reverse primers in the real-time reaction. Since the probe is sequence specific, this assay is very specific for the target sample. A less costly alternative is the SYBR Green assay. The SYBR Green dye can bind non-specifically to any double-stranded DNA and emit fluorescence. Other alternate chemistries include the molecular beacons (Stratagene, La Jolla, CA) and PCR without probes (Invitrogen, Carlabad, CA).

A typical PCR cycle consists of three primary steps. In the first melting step, the DNA to be amplified is dissociated into single strands. The primers bind specifically to the single strands during the next annealing step. Finally, the

Correspondence to: Wei-Shou Hu
Contract grant sponsor: National Institute of Health, USA
Contract grant number: GM55850-05A1

single-stranded primer complex extends into a complete double-stranded DNA molecule by addition of nucleotides during the extension step. By repeating this sequence of steps, the concentration of target DNA is increased exponentially. Under ideal conditions, the above reactions go to completion and the copies of the specific DNA sequence doubles in each cycle. In practice, the extent of the reactions depends on their rates that in turn are functions of the concentrations of reactants and enzyme.

In real-time PCR, the effect of varying reaction rates is quantified in terms of an effective efficiency, η_{eff}, such that the amount of DNA template at the end of n cycles can be related to its initial concentration by $D_{(n)} = D_{(0)}(1 + \eta_{eff})^n$. Note that η_{eff} is taken to be a constant for all the cycles. For a given value of C_T and $D_{threshold}$, knowing η_{eff} gives us $D_{(0)}$ as $D_{threshold}/(1 + \eta_{eff})^{C_T}$. η_{eff} is often obtained empirically by curve fitting to the experimental DNA concentration data (Liu and Saint, 2002a,b; Yuen et al., 2002) and assuming a constant amplification rate of the template. The extent of sequence amplification per cycle may however vary significantly over the course of PCR due to a complex interplay of different reaction rates. This may introduce error in the evaluation of η_{eff}. Analysis of the reactions involved in PCR can shed light on how different factors affect the reaction rates and thus the amplification of the DNA template.

As a reaction system, PCR has many unique features. In the course of a PCR reaction, it is not unusual that the concentration of species involved vary over several orders of magnitude. Its reactants and product concentration span over nearly ten orders of magnitude or range in opposite directions, the enzyme catalyst to substrate ratio varies in a similar fashion. The reaction cycles are carried out in a batch operation, and all reactants and enzymes are added at the beginning. In the early cycles, the molar ratios of primers and enzyme to the target DNA sequence are in the order of 10^{10} or higher. As the reactants get consumed and the target DNA concentration increases exponentially, their concentrations become comparable. The kinetic behavior of the system thus may vary rather differently under different limiting conditions. As the reaction approaches ''completion,'' at least one component in the system becomes either rate or stoichiometric limiting. The choice of the limiting factor may affect the efficiency and the accuracy of the assay. Careful analysis of the reaction system can help evaluate different scenarios and thus guide the design of experiments.

The PCR has been the subject of mathematical analysis before. Schnell and Mendoza (1997a,b) present the effect of enzyme concentration on DNA amplification. They assume melting and annealing steps to reach completion and study the extension process. Primer and nucleotide concentrations are taken to be in excess. An expression for the reaction efficiency is derived in terms of the ratio of the free to total DNA polymerase enzyme. In a similar approach, Hsu et al. (1997) study the effect of enzyme inactivation on DNA amplification. They show that DNA amplification becomes linear as the enzyme and reaction time become limiting. Stolovitzky and Cecchi (1996) present a kinetic model of the annealing and extension steps and use it to study the effect of various factors like extension time and length of DNA molecules on the DNA amplification efficiency. They also present the number of cycles for which the efficiency remains constant before decreasing to 0. Probabilistic models have also been used to describe the PCR, for example, the sequential addition of nucleotides to the single-strand primer complex has been modeled as a Markov process (Velikanov and Kapral, 1999).

In this study, we present a comprehensive model considering the kinetics of each step in detail. The stoichiometric and kinetic equations are presented in next section. Subsequently, the various kinetic parameters and operating conditions, required to simulate the process, are delineated. This is followed by simulation results under different PCR conditions. Finally, the implications to real-time PCR are discussed.

MODEL DEVELOPMENT

The model describes the specific amplification of a DNA template, referred to as D, using primers specific to this target. The sense and anti-sense primers are denoted by P and P', respectively. The chemical reactions involved in the three steps of PCR, namely, melting, annealing, and extension, are listed in Table I and are described below.

Melting

In this step, the sample is maintained at a high temperature (94–96°C). This causes the double-stranded DNA molecules to dissociate into single strands. The sense and anti-sense single-stranded DNA molecules are denoted by S and S', respectively. Apart from double-stranded target DNA, incomplete DNA molecules D_{inc} with at least one strand shorter than the template length may also be present in the sample. These molecules dissociate into incomplete single-stranded molecules S_{inc} and S'_{inc}. It is assumed that the incomplete single-stranded molecules cannot become template and therefore cannot be amplified further. However, these incomplete molecules can serve as primers to S and S' in subsequent steps. The primer dimers, R, formed by combination of primer molecules and the single-stranded template-primer complexes, also dissociate in this step. In addition, the high melting temperature causes thermal denaturation of enzyme, E, into inactivated enzyme, denoted by E_i.

Annealing

The primary reaction in this step is the annealing of the single-stranded primer molecules to the single-stranded template DNA. However, several competing reactions also occur, for example, the single-stranded templates combine with each other or with the incomplete S_{inc} and S'_{inc}. Primers may also anneal non-specifically to form primer dimers. In this step, all sense (anti-sense) single-stranded DNA templates should anneal with the corresponding primer, but

Table I. List of all reactions in real-time PCR.

(a) Melting

$$D \underset{k_{-D,m}}{\overset{k_{D,m}}{\longleftrightarrow}} S + S'$$

$$D_{\text{inc}} \underset{k_{-D,m}}{\overset{k_{D,m}}{\longleftrightarrow}} S + S'_{\text{inc}}$$

$$D'_{\text{inc}} \underset{k_{-D,m}}{\overset{k_{D,m}}{\longleftrightarrow}} S' + S_{\text{inc}}$$

$$R \underset{k_{-R,m}}{\overset{k_{R,m}}{\longleftrightarrow}} P + P'$$

$$E \xrightarrow{k_E} E_i$$

$$SP \underset{k_{-SP,m}}{\overset{k_{SP,m}}{\longleftrightarrow}} S + P$$

$$S'P' \underset{k_{-SP,m}}{\overset{k_{SP,m}}{\longleftrightarrow}} S' + P'$$

(b) Annealing

$$S + P \underset{k_{SP,a}}{\overset{k_{-SP,a}}{\longleftrightarrow}} SP$$

$$S' + P' \underset{k_{SP,a}}{\overset{k_{-SP,a}}{\longleftrightarrow}} S'P'$$

$$S + S' \underset{k_{D,a}}{\overset{k_{-D,a}}{\longleftrightarrow}} D$$

$$P + P' \underset{k_{R,a}}{\overset{k_{-R,a}}{\longleftrightarrow}} R$$

$$S + S'_{\text{inc}} \underset{k_{D,a}}{\overset{k_{-D,a}}{\longleftrightarrow}} D_{\text{inc}}$$

$$S' + S_{\text{inc}} \underset{k_{D,a}}{\overset{k_{-D,a}}{\longleftrightarrow}} D'_{inc}$$

(c) Extension

$$E + SP \underset{k_{-e}}{\overset{k_e}{\longleftrightarrow}} E \cdot SP$$

$$E \cdot SP + N \underset{k_{-n}}{\overset{k_n}{\longleftrightarrow}} (E \cdot SP \cdot N) \xrightarrow{k_{\text{cat}}} E \cdot D_1$$

$$E \cdot D_1 + N \underset{k_{-n}}{\overset{k_n}{\longleftrightarrow}} E \cdot D_1 \cdot N \xrightarrow{k_{\text{cat}}} E \cdot D_2$$

.
.

$$E \cdot D_{n-1} + N \underset{k_{-n}}{\overset{k_n}{\longleftrightarrow}} (E \cdot D_{n-1} \cdot N) \xrightarrow{k_{\text{cat}}} E \cdot D_n$$

$$E \cdot D_n \xrightarrow{k'_{\text{cat}}} E + D$$

$$\sum_{i=1}^{n-1} D_i = D_{\text{inc}}$$

$$E + S'P' \underset{k_{-e}}{\overset{k_e}{\longleftrightarrow}} E \cdot S'P'$$

$$E \cdot S'P' + N \underset{k_{-n}}{\overset{k_n}{\longleftrightarrow}} (E \cdot S'P' \cdot N) \xrightarrow{k_{\text{cat}}} E \cdot D'_1$$

$$E \cdot D'_1 + N \underset{k_{-n}}{\overset{k_n}{\longleftrightarrow}} (E \cdot D'_1 \cdot N) \xrightarrow{k_{\text{cat}}} E \cdot D'_2$$

.
.

$$E \cdot D'_{n-1} + N \underset{k_{-n}}{\overset{k_n}{\longleftrightarrow}} (E \cdot D'_{n-1} \cdot N) \xrightarrow{k_{\text{cat}}} E \cdot D'_n$$

$$E \cdot D'_n \xrightarrow{k'_{\text{cat}}} E + D'$$

$$\sum_{i=1}^{n-1} D'_i = D'_{\text{inc}}$$

$$E + R \underset{k_{-e}}{\overset{k_e}{\longleftrightarrow}} E \cdot R$$

$$E \cdot R + nN \underset{k_{-n}}{\overset{k_n}{\longleftrightarrow}} (E \cdot R \cdot nN) \xrightarrow{k'_{\text{cat}}} E + R_n$$

not with the anti-sense (sense) single-stranded DNA. Also, for 100% efficiency, no single-stranded template should be left unannealed. This can be achieved by having primers in excess to drive the single-stranded template to form primer–template complex. Alternatively, the reaction conditions can be chosen such that the reaction rate for primer-template duplex formation is much greater than that for annealing of single-stranded template.

Extension

In the extension step, the polymerase enzyme, E, binds to the single-stranded template-primer complex, SP and extends it by the addition of a nucleotide, N, to form $E \cdot D_1$. Another nucleotide is added in a similar way to yield $E \cdot D_2$. This stepwise reaction is repeated until n nucleotides are added to form the full-length $E \cdot D_n$ complex, which then dissociates to form the complete DNA template. Note that $D_n = D$. All the incomplete double-stranded molecules, formed from $E \cdot D_i$ for $i = 1,\ldots, n-1$, are collectively denoted as D_{inc}. The extension of the anti-sense complex, $S'P'$, follows analogous steps. The enzyme extending SP and $S'P'$ to form D (Table I) is assumed to be fully processive that does not dissociate after the addition of each nucleotide. Most DNA polymerase enzymes are processive where once bound, they can add more than 200 nucleotides before dissociating (Einolf and Guengerich, 2000; Lowe and Guengerich, 1996). In addition, for the short templates typical of quantitative PCR, the nucleotide incorporation error rate is expected to be negligible. We thus also assume 100% fidelity in template replication. Any $E \cdot D_i$ for $i=1,\ldots, n$, complex at the end of extension is assumed to dissociate into free enzyme and D_i molecules at the beginning of subsequent melting step.

The differential equations for time evolution of species concentrations in the above three steps are listed in Table II. We assume mass-action type kinetics for all reactions. The kinetic equations for nucleotide addition are further simplified by assuming quasi-steady state for each of the intermediates $E \cdot T \cdot N$ where $T = SP,\ D_1,\ldots,D_{n-1}$. The concentration of $E \cdot T \cdot N$ can thus be derived in terms of the concentration of $E \cdot T$ as $[E \cdot T \cdot N] = [E \cdot T][N]/K_N$ where K_N is the Micheles–Menton constant (see appendix for details).

SIMULATION PARAMETERS

To simulate the PCR using the equations listed in Table II, various parameters including the reaction rate constants and the initial concentrations of DNA template, primers, nucleotide, and DNA polymerase enzyme were estimated from literature reported values. The operating conditions like melting, annealing, and extension cycle times used are also typical values reported in literature. These parameters and their values are listed in Table III and described below.

Denaturation

The rate constants of DNA denaturation and renaturation are functions of the operating temperature, and the length and homology of the DNA molecules. For short DNA, denaturation can be assumed to be a first order process, where at any

Table II. Kinetic equations for PCR.

(a) Melting

$$\frac{d[S]}{dt} = 2 * k_{D,m}[D] - k_{-D,m}[S]^2 + k_{D,m}[D_{inc}] - k_{-D,m}[S] \cdot [S_{inc}] - k_{-SP,m}[S][P] + k_{SP,m}[SP]$$

$$\frac{d[S_{inc}]}{dt} = k_{D,m}[D_{inc}] - k_{-D,m}[S] \cdot [S_{inc}]$$

$$\frac{d[P]}{dt} = +2k_{R,m}[R] - k_{-R,m}[P]^2 - k_{-SP,m}[S][P] + k_{SP,m}[SP]$$

$$\frac{d[E]}{dt} = -k_E E$$

$$\frac{d[SP]}{dt} = k_{-SP,m}[S][P] - k_{SP,m}[SP]$$

$$\frac{d[D]}{dt} = \tfrac{1}{2}k_{-D,m}[S]^2 - k_{D,m}[D]$$

$$\frac{d[D_{inc}]}{dt} = k_{-D,m}[S] \cdot [S_{inc}] - k_{D,m}[D_{inc}]$$

$$\frac{d[R]}{dt} = \tfrac{1}{2}k_{-R,m}[P]^2 - k_{R,m}[R]$$

(b) Annealing

$$\frac{d[SP]}{dt} = k_{-SP,a}[S][P] - k_{SP,a}[SP]$$

$$\frac{d[S]}{dt} = -k_{-SP,a}[S][P] + k_{SP,a}[SP] - k_{-D,a}[S]^2 + 2k_{D,a}[D] - k_{-D,a}[S][S_{inc}] + k_{D,a}[D_{inc}]$$

$$\frac{d[P]}{dt} = -k_{-SP,a}[S][P] + k_{SP,a}[SP] + 2k_{R,a}[R] - k_{-R,a}[P]^2$$

$$\frac{d[R]}{dt} = \tfrac{1}{2}k_{-R,a}[P]^2 - k_{R,a}[R]$$

$$\frac{d[D]}{dt} = \tfrac{1}{2}k_{-D,a}[S]^2 - k_{D,a}[D]$$

$$\frac{d[S_{inc}]}{dt} = -k_{-D,a}[S][S_{inc}] + k_{D,a}[D_{inc}]$$

$$\frac{d[D_{inc}]}{dt} = k_{-D,a}[S][S_{inc}] - k_{D,a}[D_{inc}]$$

(c) Extension

$$\frac{d[D_n]}{dt} = k'_{cat} \cdot [E \cdot D_n]$$

$$\frac{d[E \cdot D_n]}{dt} = k_{cat}\frac{[E \cdot D_{n-1}][N]}{K_N} - k'_{cat} \cdot [E \cdot D_n]$$

$$\frac{d[E \cdot D_1]}{dt} = k_{cat}\frac{[E \cdot SP][N]}{K_N} - k_{cat}\frac{[E \cdot D_1][N]}{K_N}$$

$$\frac{d[E \cdot T_i]}{dt} = k_{cat}\frac{[E \cdot T_{i-1}][N]}{K_N} - k_{cat}\frac{[E \cdot T_i][N]}{K_N}$$

where $T = D_1, \ldots, D_{n-1}$

$$\frac{d[E \cdot SP]}{dt} = k_e[E] \cdot [SP] - k_{-e}[E \cdot SP] - k_{cat}\frac{[E \cdot SP][N]}{K_N}$$

$$\frac{d[SP]}{dt} = k_{-e}[E \cdot SP] - k_e \cdot [E][SP]$$

$$\frac{d[N]}{dt} = \frac{k_{cat}[N]\left(\sum_{T=SP}^{D_{n-1}}[E \cdot T]\right)}{K_N}$$

given temperature, completely melted single strand and helix duplex coexist in equilibrium. At low temperatures, all DNA exists in duplex form whereas the DNA is completely dissociated into single strands at high temperatures. The transition between these two states has been reported to span 2–4°C (Wartell and Benight, 1985), with the midpoint denoted as melting temperature, T_m. The sharpness of this transition depends on the length of the DNA molecule and other factors such as ionic strength.

For complete melting, the temperature used is higher than T_m. A high temperature in the range 94–96°C, depending on the composition (GC content, etc.) of the DNA template, is generally used. At these temperatures, the denaturation rate constant $k_{D,m}$ for a DNA molecule of length L, can be calculated as $2{,}500/L \cdot s$, based on a rate constant of 250/s for ~10 bp long oligomer (Breslauer and Bina-Stein, 1977; Record, 1972). The annealing temperature is suggested to be approximately 5–8°C below the melting temperature of primers (Qiagen, 2002a). This is about 25°C below the melting temperature of D. Denaturation time increases sharply as temperature is lowered. Therefore, the melting rate for D at annealing temperature $k_{D,a}$ is orders of magnitude lower than the corresponding rate in the melting step. We use a value of 10^{-4}/s as reported in literature (Gotoh et al., 1995; Jensen et al., 1997). The same rate constant is assumed for the dissociation of the SP complex $k_{SP,a}$.

The denaturation rate is higher for non-homologous DNA than that for completely homologous DNA. Anderson and Young (1985) report that the duplex dissociation rate increases by a factor of 2 for every 10% mismatch of the single-stranded sequences. Primer dimers would in general have a significant mismatch. At melting temperature, the rate constant of a perfectly matched primer duplex with $L = 20$, can be estimated to be $2{,}500/L \cdot s = 125$/s. With the mismatch in primer dimers, the value would be much higher, we thus use a dissociation rate constant $k_{R,m} = 1.25 \times 10^4$/s. At annealing temperature, the corresponding rate constant $k_{R,a}$ is taken to be 10^{-2}/s, which is 100 times higher than $k_{D,a}$.

Renaturation

The process of renaturation consists of two main steps, nucleation and zipping. Nucleation is the rate-limiting step, whereas the zipping reaction is very fast. The renaturation rate constant for single strands of equal lengths $k_{-D,a}$ is taken to be 1×10^6/M · s at annealing temperature (Craig et al., 1971). For renaturation of single strands of primer and template to form the SP complex, the annealing rate is assumed to be proportional to the square root of length of the shorter strand (Wetmur and Davidson, 1968). The rate constant $k_{-SP,a}$ is therefore about 1/2 $k_{-D,a}$. Primer dimer formation is principally non-specific in nature. Therefore, the corresponding rate constant $k_{-R,a}$ is taken to be two orders of magnitude lower than $k_{-SP,a}$. Studies have shown that the renaturation rate is only a modest function of temperature (Breslauer and Bina-Stein, 1977; Craig et al., 1971). Therefore, identical rate constants are used for the melting step. Specifically, $k_{-D,m}$, $k_{-R,m}$, and $k_{-SP,m}$ are taken to be equal to $k_{-D,a}$, $k_{-R,a}$, and $k_{-SP,a}$, respectively.

Enzyme Inactivation

The DNA polymerase enzyme may be inactivated at high temperatures. The half-life of various DNA polymerase enzymes is found to vary between 9 and 130 min for a temperature range 92–97°C (Qiagen, 2002b). The higher value corresponds to a temperature of 92°C and the lower value is for a temperature of 97°C. We use a half-life of 60 min to obtain the enzyme inactivation rate constant k_E as 1.9×10^{-4}/s.

Table III. Simulation parameters for the PCR model.

Parameters	Description	Value
$k_{D,m}$	Denaturation constant for melting of double-stranded homologous DNA of length L bps at melting temperature	$2{,}500/L \cdot s$
$k_{-D,a}$, $k_{-D,m}$	Renaturation constant for binding of single-stranded DNA at annealing and melting temperature	$10^6/M \cdot s$
$k_{D,a}$	Denaturation constant for melting of 100 bp double-stranded DNA at annealing temperature	$10^{-4}/s$
k_E	Enzyme inactivation constant	$1.9 \times 10^{-4}/s$
$k_{R,m}$	Dissociation of the primer dimer at melting temperature	$1.25 \times 10^4/s$
$k_{-SP,a}$, $k_{-SP,m}$	Annealing of primer to single strand	$5 \times 10^5/M \cdot s$
$k_{SP,a}$	Dissociation of the SP complex	$10^{-4}\ s^{-1}$
$k_{R,a}$	Dissociation of the primer dimer at annealing temperature	$10^{-2}/s$
$k_{-R,a}$, $k_{-R,m}$	Specific/non-specific annealing of primers to form primer-dimers at annealing and melting temperature	$5 \times 10^3/M \cdot s$
k_e	Addition of enzyme to SP complex	$10^8/M \cdot s$
k_{-e}	Dissociation of enzyme from SP.E complex	10/s
K_N	Micheles–Menton constant for nucleotide addition	4 μM
K_s^D	Dissociation constant for the complex of enzyme and single-stranded substrate	100 nM
k_{cat}	Rate of nucleotide addition	60/s
k'_{cat}	Release of double-stranded product from enzyme	10/s
t_{melt}	Melting cycle time	15 s
t_{anneal}	Annealing cycle time	30 s
t_{extn}	Extension cycle time	30 s
L	Length of DNA template	100 bp
L_{p}	Length of primer	20 bp

DNA Extension

For the extension of the primer–template complex, the kinetic constants were estimated for the Taq DNA polymerase enzyme. The equilibrium dissociation constant for the DNA–enzyme complex K_s^D is reported to be 103 nM at 70°C (Datta and LiCata, 2003). We estimate the forward rate constant for enzyme-DNA binding k_e as $10^8/M \cdot s$. The dissociation rate constant k_{-e} of the DNA–enzyme complex is therefore taken to be 10/s. The Micheles–Menton constant for nucleotide incorporation K_N has been measured as 2.2–9.1 μM depending on which nucleotide is being added (Tosaka et al., 2001). We take an average value of 4 μM. The extension rate k_{cat} for Taq is taken to be 60/s, which is in the range reported (Qiagen, 2002b). The dissociation of the $E \cdot D_n$ complex k'_{cat} is assumed to be equal to k_{-e}.

Initial Concentrations and Cycle Times

The length of the target DNA and primers is taken to be 100 and 20 bp, respectively. The total reaction volume is taken as 50 μL. Initial concentrations of primers (P_0), nucleotide (N_0), template ($D_{(0)}$), and enzyme (E_0) are typical of a real-time PCR. The values used in the simulations are listed in the next section.

The recommended melting time is generally about 15–60 s (Qiagen, 2002a), to raise the temperature of the reaction mixture to desired value. We use a value of 15 s. Annealing time is taken to be 30 s that lies in the suggested range (Qiagen, 2002a). The optimum extension temperature is about 72°C. At this temperature, the extension time is calculated to be 30 s based on the length of the DNA template and the k_{cat} for DNA polymerase enzyme.

Simulation Results

The model and kinetic parameters presented above were used to simulate typical PCR kinetics. First, we present an ideal case to obtain the minimum concentration (stoichiometric concentrations) of primer, nucleotide, and enzyme required for a given initial template concentration. Next, we investigate the reaction kinetics where the PCR is stoichiometrically limited by primer, nucleotide, and enzyme respectively. This is followed by simulation of typical experimental conditions, where the effect of primer dimerization and DNA rehybridization on the reaction efficiency are discussed.

We assume both the sense and anti-sense single-stranded DNA species to be essentially the same. Similarly, the sense and anti-sense primers and the four different nucleotides are not distinguished. The melting, annealing, and extension are treated as three distinct steps in succession, where each step is integrated for the respective cycle time (Table III). The final concentration obtained from one step is treated as the initial condition for the next step. It is further assumed that the time to change the temperature between different steps (ramp time) is negligible compared to the individual step time. The whole cycle of three steps is repeated to simulate over 40 cycles. Cycle efficiency for ith cycle, η_i, is defined as

$$\eta_i = \frac{D_{(i)} - D_{(i-1)}}{D_{(i-1)}}$$

where $D_{(i)}$ is the template concentration at the end of ith cycle.

Stochiometric Requirements

Melting and annealing steps during PCR consist of the following reactions:

$$D \underset{k_{-D,m}}{\overset{k_{D,m}}{\longleftrightarrow}} S + S'$$

$$SP \underset{k_{-SP,m}}{\overset{k_{SP,m}}{\longleftrightarrow}} S + P$$

$$S' + P' \underset{k_{-SP,m}}{\overset{k_{SP,m}}{\longleftrightarrow}} S' + P'$$

that go to completion. In an ideal case, the other reactions listed in Table Ia and b are neglected. It is further assumed that all the substrate–primer complexes (SP and $S'P'$) are completely extended to form D, that is, $D_{\text{inc}} = 0$. Therefore, each cycle doubles the amount of target DNA such that at the end of n cycles, the amount of double–stranded product is $D_{(n)} = S_{(0)}2^n$, where $D_{(0)}$ is the initial template concentration.

The corresponding stoichiometric initial concentrations of primer (sense and anti-sense) and nucleotides are given by

$$P_{\text{stoic}} = D_{(0)}(2^{n+1} - 2) \approx D_{(0)}2^{n+1}$$

$$N_{\text{stoic}} = D_{(0)}(2^{n+1} - 2)(L - L_p) \approx D_{(0)}2^{n+1}(L - L_p)$$

respectively. Here L is the length of template in base pairs and L_{p} refers to the primer length. The stoichiometric enzyme concentration is the amount sufficient for the extension reaction in the nth cycle, where t_{extn} is the extension cycle time and k_{cat} represents the nucleotide addition rate.

$$E_{\text{stoic}} = \frac{D_{(0)}2^n(L - L_{\text{p}})}{k_{\text{cat}}t_{\text{extn}}}$$

Figure 1 shows P_{stoic}, N_{stoic}, and E_{stoic} as a function of initial amount of template and cycle number. This corresponds to the minimum amount of primer, nucleotide, and enzyme required for a given $D_{(0)}$ and n. The recommended concentrations in experimental protocols are also shown in the respective plots. For these values, the number of cycles that can be achieved under ideal conditions for a given $D_{(0)}$ can thus be computed. For example, for $D_{(0)} = 10^{-10}$ μM, the recommended concentrations of primer and enzyme are sufficient for 25 cycles, whereas the nucleotide can last up to 35 cycles.

Primer, Nucleotide, and Enzyme Limiting Conditions

We simulate PCR kinetics under primer, nucleotide, and enzyme limiting conditions, respectively, for $D_{(0)} = 3.32 \times 10^{-6}$ nM (10^5 copies in 50 μL). The initial concentration

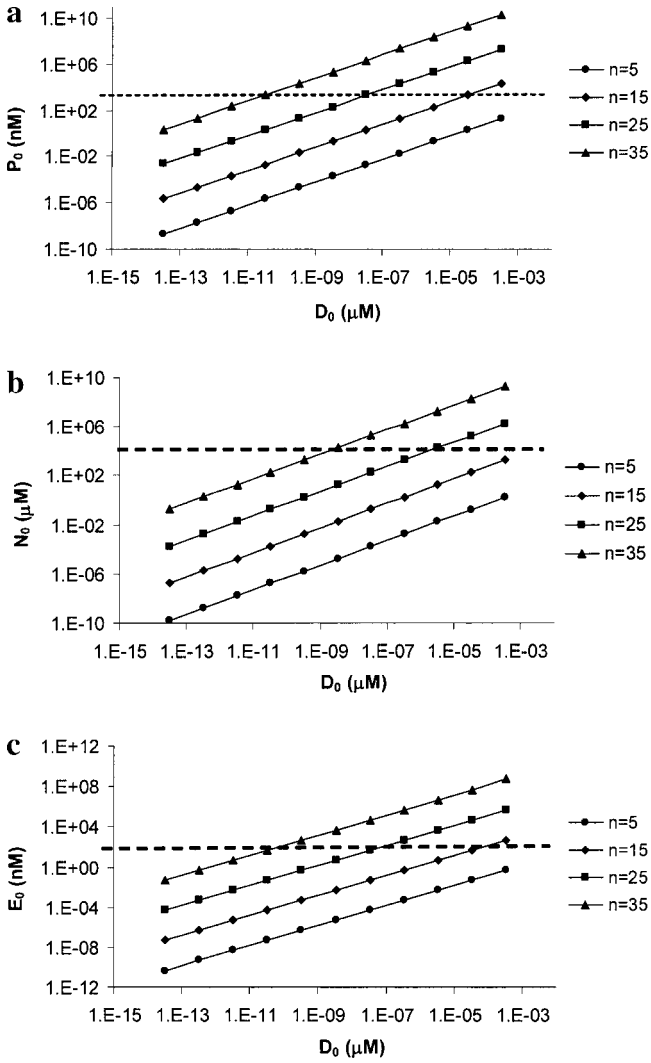

Figure 1. Stoichiometric concentrations of (**a**) primer, (**b**) nucleotide, and (**c**) enzyme as a function of initial template concentration (D_0) and cycle number (n). The dashed lines correspond to concentrations used in typical reactions as recommended by vendors.

of the limiting species is taken to be equal to the corresponding stoichiometric value for 25 cycles ($P_{\text{stoic}} = 0.223$ μM, $N_{\text{stoic}} = 17.8$ μM, and $E_{\text{stoic}} = 4.95$ nM). The rest of the reactants in each case are in excess and their initial concentrations are 100 times the respective stoichiometric values.

Figure 2a shows the kinetic progression of the DNA template and the consumption of primers, nucleotide, and enzyme for the primer limiting condition. All the concentrations are normalized by the corresponding stoichiometric values. The amplification efficiency at each cycle is also shown. The nucleotide and enzyme concentration are essentially constant during the simulation. Three distinct phases can be seen in the kinetic curve of template and primer concentrations. Initially, there is enough primer to cause exponential amplification of the template with an efficiency of 1 ($D_{(n)} = D_{(0)}2^n$). Next, there is a rapid decrease in the primer concentration in the transition phase ($20 < n < 30$). The amount of SP formed in the annealing step is pro-

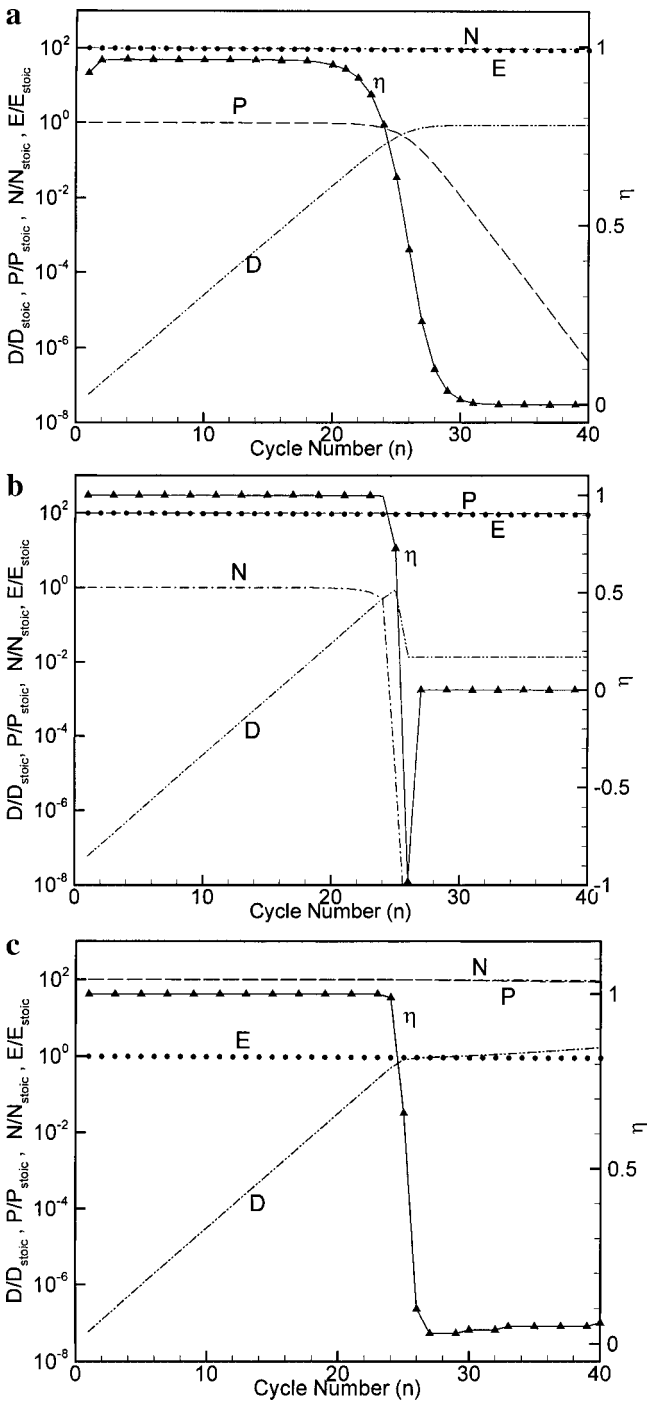

Figure 2. PCR kinetics under (**a**) primer, (**b**) nucleotide, and (**c**) enzyme limiting conditions, respectively. All concentrations are normalized to respective stoichiometric value for 25 cycles. Initial concentration of the rate limiting species is taken to be equal to the corresponding stoichiometric value for $D_0 = 3.32 \times 10^{-6}$ nM and 25 cycles. The rest of the reactants are in excess and their initial concentrations are 100 times the respective stochiometric values.

portional to the concentrations of *S* and *P*. In the early cycles, *P* is in excess, thus driving all *S* to form *SP*. As the concentrations of *P* and *S* become comparable, not all of the single-stranded template *S* may get converted to *SP*. Therefore, the rate of template formation reduces and efficiency is lower than 1. Finally, all the primer is used up to reach a plateau phase where *D* is constant and efficiency is close to zero.

For the nucleotide limiting condition, the enzyme and primer concentrations remain in excess during the entire simulation period of 40 cycles. Initially, the nucleotide concentration does not change appreciably, accompanied by an exponential increase in *D*. Subsequently, *N* decreases rapidly to go down to 0 within few cycles. Low values of *N* limit the extension reactions that form *D* from *SP*. This leads to a decrease in DNA concentration of two orders of magnitude (see Fig. 2b). The efficiency remains at a high value ($\eta > 0.98$) for $20 < n < 25$ when the nucleotide concentration decreases by an order of magnitude. This is in contrast to the primer limiting case, where η decreases to 0.1 for a similar drop in *P*. This is because as long as *N* is greater than K_N, the template extension rate is close to its maximum value. For a K_N value of 4 μM used in this simulation, *N* is $\gg K_N$ even at $n = 25$.

Another major difference between the primer and nucleotide limiting cases is the variation in template concentration in the later part of the simulation. Once the nucleotides are depleted, the existing DNA molecules dissociate in the subsequent melting step. The single strands thus formed anneal with the primers, which are in excess to form *SP* complexes. The *SP* molecules cannot extend to form *D* due to lack of nucleotide. This results in a decrease in the overall DNA level. By comparison, the template concentration reaches a plateau in the primer limiting case.

Figure 2c shows the results from the enzyme-limiting simulation. The concentrations of nucleotide, primer, and enzyme remain essentially constant. Initially, the DNA concentration shows an exponential growth. As the DNA concentration rises, the enzyme requirement also increases. At $n = 25$, the enzyme concentration becomes limiting, and the template amplification rate decreases markedly.

Inverse Effect of Primer Concentration

The simulations presented above set one reactant at the stoichiometrically limiting level while others at levels two orders of magnitude in excess. Under typical experimental conditions, all the reactant concentrations are close to their stoichiometric values. Therefore, under typical experimental conditions, the observed time profiles of template concentration may differ from the simulations presented above. Typical PCR conditions are simulated with initial reactant concentrations in the range of recommended values. The concentration of primer is varied between 0.2 and 2 μM, while total nucleotide and enzyme concentrations are set at 800 μM and 2.5 nM, respectively. These values result in primer and/or enzyme-limiting conditions around cycle number 25 for initial template concentration ($D_{(0)}$) of 3.32×10^{-6} nM. The simulation results are presented in Figure 3, which shows the amplification of template DNA concentration over 40 cycles for varying primer concentrations. As P_0 increases from 0.2 to 1 μM, the final template

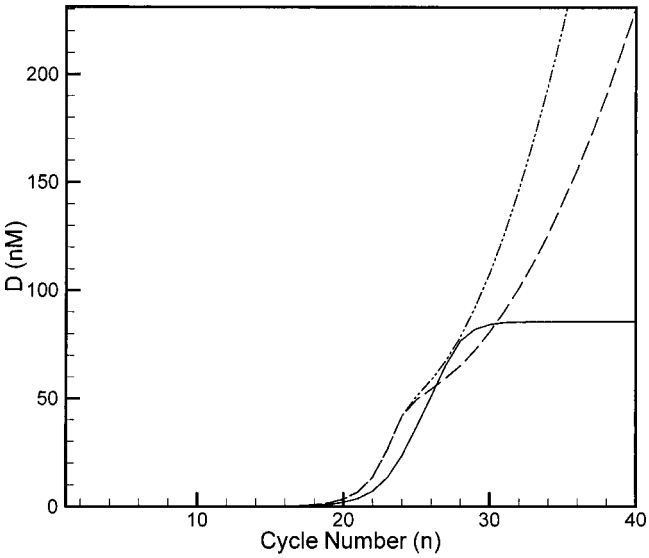

Figure 3. Template DNA concentration as a function of cycle number for primer concentrations of 2 μM (– – -), 1 μM (– · · –), and 0.2 μM (—). Initial concentrations of the rest of the species correspond to typical PCR experiment.

DNA concentration increases. However, further increase of primer concentration to 2 μM results in a reduced final template DNA concentration. This effect of primer concentration has been observed experimentally (Ponchel et al., 2003). Such a sensitivity of PCR results to the primer concentration can cause significant error in the estimation of initial template concentration.

A closer scrutiny of the kinetic behavior of the intermediates reveals that the inverse effect of primer concentration occurs in the region where enzyme becomes stoichiometrically limiting. Under such conditions, the extension reaction of elongating *SP* complex has reached its maximum rate (assuming primer and nucleotide are not limiting). Thus, the amount of template duplex generated from the extension reaction is constant regardless of higher *SP* concentration for P_0 of 2 μM. In other words at both P_0 concentrations of 1 and 2 μM, the same amounts of *D* are formed by the extension of *SP*. In addition to template DNA molecules formed in the extension step, at some concentrations of excess *S*, dimerization of *S* during annealing also result in duplex *D* that contributes to the total concentration of *D* detected. The formation of *D* from *S* is subjected to competition from the primers in the reaction mixture. A higher P_0 may give rise to conditions that reduce single-stranded reannealing to form *D*, thus resulting in the overall lower concentration of template DNA. This inverse effect of increasing primer concentration on template formed is thus limited to conditions in which enzyme is stoichiometrically limiting.

Effect of Primer Dimerization

At high concentrations, primers may bind to one another nonspecifically to form primer dimers. Such side reactions consume primer and reduce the amount available for template amplification. If the dimers contribute to fluorescence, it also leads to errors in determining C_T value. We consider two types of primer dimers. The first kind does not extend. They dissociate at subsequent melting and can be reused in the next annealing step. The other extend and their sequence becomes non-specific, making them incapable of priming in subsequent cycles. The real mechanism will be some combination of the above cases.

Figure 4a shows the reaction efficiency as a function of cycle number for the two kinds of primer-dimers. The results from a simulation without primer-dimers are also shown for comparison. P_0 is taken to be 0.2 μM. For the case that primer-dimers do not extend the time profile of efficiency is

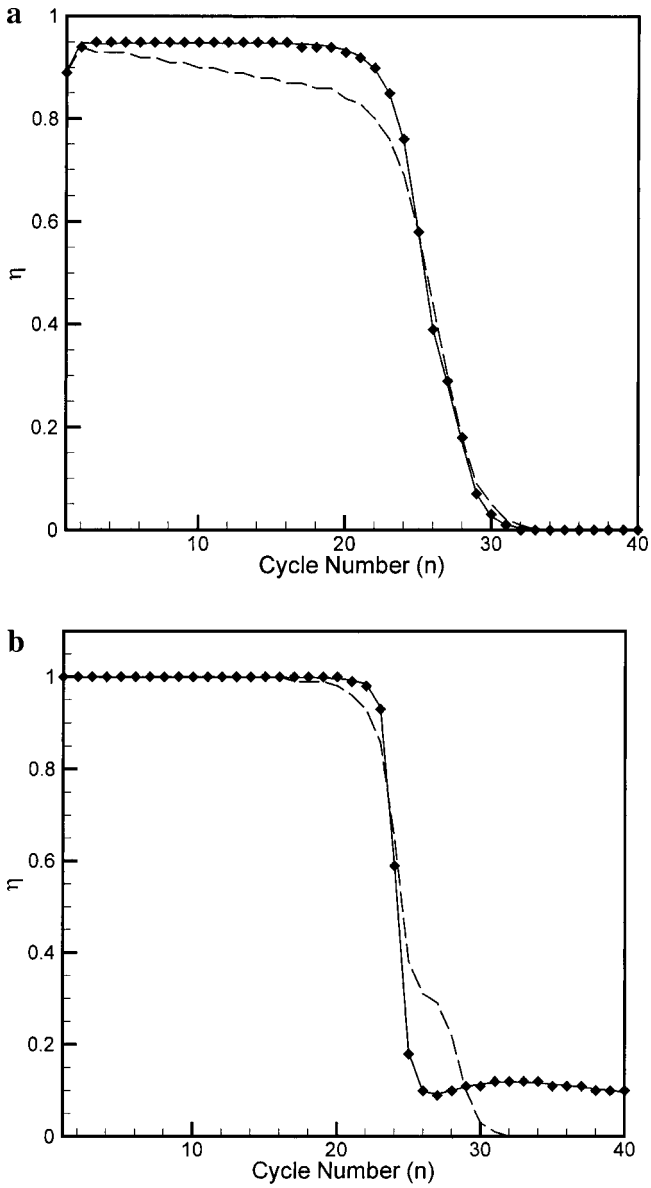

Figure 4. Variation of reaction efficiency with cycle number in simulations with no primer dimer formation (—), primer dimers that cannot extend (◆), and primer dimers that can extend (– – –): (**a**) $P_0 = 0.2$ μM, (**b**) $P_0 = 2$ μM. The curves for $P_0 = 1$ μM are similar to those for $P_0 = 2$ μM. Initial concentrations used in the simulations are typical of a PCR experiment.

identical to that of no primer-dimer formation. By comparison, the second kind of primer-dimers decrease the concentration of free primers available to anneal with single strands of DNA resulting in gradual reduction of the reaction efficiency. The effect of primer dimers on the reaction efficiency varies with the initial primer concentration. In contrast to $P_0 = 0.2$ μM, primer dimerization does not affect the efficiency until 15 cycles for P_0 of 1 μM and higher (see Fig. 4b). This is because inspite of primer dimerization, the primer concentration is in excess during these cycles. Also, there is an increase in efficiency due to primer dimerization beyond cycle number 24 for $P_0 = 1$ and 2 μM and a shoulder is observed around cycle number 26. The observed plateau in reaction efficiency at cycle number 26 corresponds to the transition from enzyme limiting to primer limiting conditions. Due to enzyme limitation, *SP* complex cannot extend to form *D* during the extension step and hence start accumulating at the end of cycle number 24. However as primer becomes limiting, less amount of *SP* complex is formed for these cases. At cycle number 26, the amount of enzyme available is therefore enough for extension of all *SP* into *D*, resulting in higher efficiency. The reaction rate constant for primer dimerization, $k_{-R,a}$ is taken to be 5×10^3/M · s. If $k_{-R,a}$ is an order of magnitude higher, template amplification is greatly reduced when the primer dimers can extend and become unusable. The reaction efficiency is also affected when the primer dimers cannot extend. Sensitivity of the model to the other reaction rate constants was also examined. Variation in $k_{-D,a}$ and $k_{-SP,a}$ decreases the maximum efficiency for P_0 of 0.2 μM. An increase in the half-life of the Taq DNA polymerase causes appreciable decrease in the efficiency during the later cycles. A similar effect is observed on decreasing the k_{cat}.

Effect of DNA Rehybridization on Reaction Efficiency

Critical to the efficiency is the complete conversion of *S* to *SP* duplex through the primary reaction in the annealing step: $S + P \rightarrow SP$. However, the single strand *S* can reanneal to form *D* through the competing reaction: $S + S \rightarrow D$. Any *S* that fails to form *SP* will not be amplified in the elongation step, thus reducing the amplification of the template. This has been cited as a major reason for the decrease in the reaction efficiency (Mathieu-Daude et al., 1996). Figure 5 shows the fraction of *S* present at the beginning of annealing that becomes primer-template duplex at the end of the step (SP_f/S_b) as a function of the ratio P_b/S_b and P_b. Here subscripts *b* and *f* represent the concentrations at the beginning and end of the annealing step. We are interested in only the experimentally relevant region where $(P_b/S_b) > 1$. For the accurate quantification of initial template concentration, a constant and perfect efficiency is most desirable. Thus SP_f/S_b should be close to 1. It is clear that the primer being present at a simple stoichiometric excess is not sufficient to achieve high efficiency; as at a P_b/S_b ratio of 5, only 80% of S_b will form *SP*. A large excess of primer ($P_b \gg S_b$) along

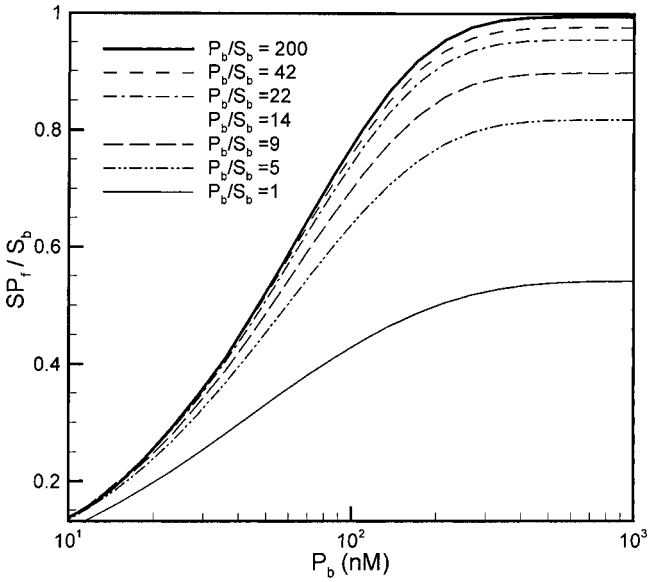

Figure 5. The fraction of *S* converted to *SP* in an annealing step as a function of primer concentration for varying P_b/S_b ratios.

with high primer concentrations are essential for the *SP* formation reaction to dominate and achieve SP_f/S_b close to 1. The variation of SP_f/S_b over 40 cycles for the typical experimental conditions described above is presented in Figure 6. The ratio is close to 1 for the initial cycles, and it decreases as the primer concentration becomes limiting. The efficiency of the reaction is also plotted, and we see a strong correlation of η with SP_f/S_b.

COMPARISON WITH EXPERIMENTAL RESULTS

PCR reactions were carried out to simulate primer, nucleotide, and enzyme limiting conditions by varying concentrations

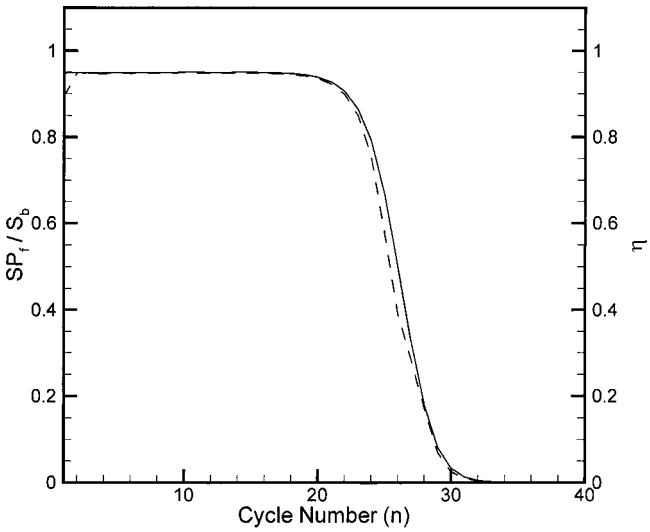

Figure 6. Effect of single-stranded rehybridization: the fraction SP_f/S_b (—) and cycle efficiency (– – –) are plotted as a function of cycle number. The simulation corresponds to typical experimental conditions with $P_0 = 0.2$ μM.

of primer, nucleotide, and enzyme, respectively. The *hrdB* gene of *Streptomyces coelicolor* was chosen as the target gene. Forward and reverse primers were designed by Primer3 (http://frodo.wi.mit.edu/) for an amplicon size of 200 bp. Agarose gel electrophoresis was used to confirm the amplicon size. Real-time analysis was performed on ABI7700 (Applied Biosystems, Foster City, CA).

The reaction mixture of a 12-µl final volume contained 1 × SYBR® Green Dye (Invitrogen), 50 ng of genomic DNA template, 1.2 µL DMSO, 1.2 µL glycerol, 1× PCR buffer, 2.5 mM $MgCl_2$ and milliQ water in addition to primers, nucleotide, and enzyme. Stoichiometric concentration of primer and nucleotide for 18 cycles was calculated as 0.4 and 70 µM, respectively. The concentration of total sense and anti-sense primers was 0.4 µM for the primer limiting case and 2 µM otherwise. For nucleotide limiting conditions, 70 µM of total dNTPs were used. Nucleotide concentration was 800 µM for primer and enzyme limiting cases. To estimate the limiting concentration of enzyme, Platinum Taq DNA polymerase (Invitrogen) was varied from 0.05 to 10 U. Enzyme (0.5 U) was used for enzyme limiting case, whereas 2 U correspond to enzyme in excess. A no template control (NTC) was included to check for the formation of primer-dimers. PCR conditions were as follows: initial denaturation at 95°C for 15 min followed by 40 cycles of 94°C for 20 s, 60°C for 30 s, and 72°C for 15 s. To check the specificity of the real-time PCR reaction, a DNA melting curve analysis was performed by holding the sample at 60°C for 60 s followed by slow ramping of the temperature to 95°C. The specificity of the PCR product was confirmed by the single peak in the dissociation curve and the absence of any significant amplification in the NTC.

Fluorescence intensity was collected at the end of each extension step. This was used to calculate the reaction efficiency at each cycle as defined below:

$$\eta_i = \frac{(F_{(i)} - F_{(i-1)})}{F_{(i-1)}}$$

where $F_{(i)}$ is the fluorescence intensity at the end of *i*th cycle. Figure 7 illustrates the reaction efficiency for three different combinations of primer, nucleotide, and enzyme. These correspond to primer, nucleotide, and enzyme limiting conditions, respectively. Reaction efficiency is calculated only for cycles where fluorescence is above the detection limit. Cycle number is relative to the cycle where signal is detected. Simulation results predict a constant efficiency region followed by a decrease in efficiency as one of the reactant becomes limiting, as shown in Figure 2. The drop in efficiency is steeper when either nucleotide or enzyme is limiting, as compared to when primer is limiting (Fig. 2). Experimental results corroborate this prediction. Note that the maximum reaction efficiency and the slope of the efficiency transition kinetics are dependent on the kinetic parameters. The value of many parameters, including the annealing rate for single strand and primers, cannot be precisely estimated. Nevertheless, the general trends obtained from experimental data are comparable to the theoretical predictions.

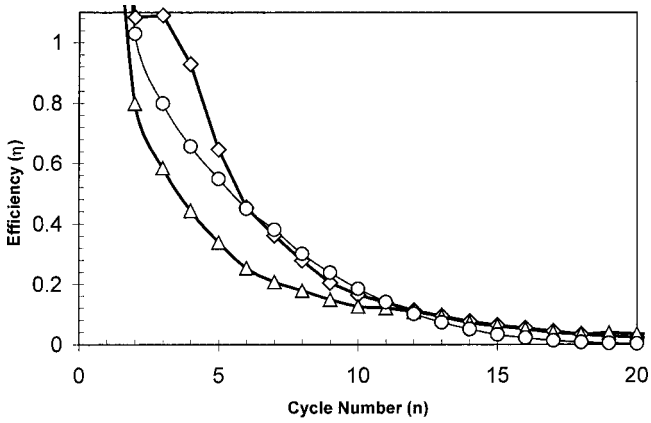

Figure 7. Plot of experimentally determined real-time PCR reaction efficiencies as a function of cycle number. Cycle number is relative to the cycle where signal is detected. The three curves correspond to primer limiting (○), nucleotide limiting (◇), and enzyme limiting (△) conditions. The initial concentration of primer, nucleotide and enzyme for the three cases are as follows: Primer limiting: $P_0 = 0.4$ µM, $N_0 = 800$ µM, $E_0 = 2$ U; Nucleotide limiting: $P_0 = 2$ µM, $N_0 = 70$ µM, $E_0 = 2$ U; and Enzyme limiting: $P_0 = 2$ µM, $N_0 = 800$ µM, $E_0 = 0.5$ U, respectively. Each curve is an average over three replicates.

IMPLICATION FOR REAL-TIME PCR APPLICATIONS

In real-time PCR, the concentration of DNA is detected by a fluorescent dye that binds to double-stranded DNA. The detection limit of the fluorescent signal dictates the minimum concentration of DNA that can be measured. Above the detection limit, the fluorescence intensity increases linearly with the DNA concentration over a range before approaching the saturation level. Using a system employing SYBR Green dye as an example, the reported minimum detection limit of ~2 ng/ml (Rengarajan et al., 2002) gives a linear fluorescent response up to 10–20 ng of DNA per 5 µL reaction mixture (Wittwer et al., 1997). Thus for a 100 bp product, the detectable concentration range is 31 pM–60 nM where fluorescence is proportional to the DNA concentration. The threshold level to determine C_T should lie in this linear detection range. Simulations using typical PCR conditions for a P_0 of 0.2 µM are shown in Figure 8. Two vertical lines mark the linear detection range described above. Setting $D_{\text{threshold}}$ as 10 nM yields a C_T value of 22.5. $D_{(0)}$ can then be computed as $D_{\text{threshold}}/(1+\eta_{\text{eff}})^{C_T}$.

The standard curve method is commonly used to obtain η_{eff}. A standard curve is generated by plotting C_T values of different dilutions samples versus the logarithm of their known initial concentrations. The efficiency is then obtained from the slope of the curve. Using the conditions listed above, we constructed a standard curve for a $D_{(0)}$ range of 332–3.32×10^{-11} nM and a $D_{\text{threshold}}$ of 10 nM, to obtain an efficiency of 0.95. A second method fits an exponential curve through the kinetic profile of the intensity (or the concentra-

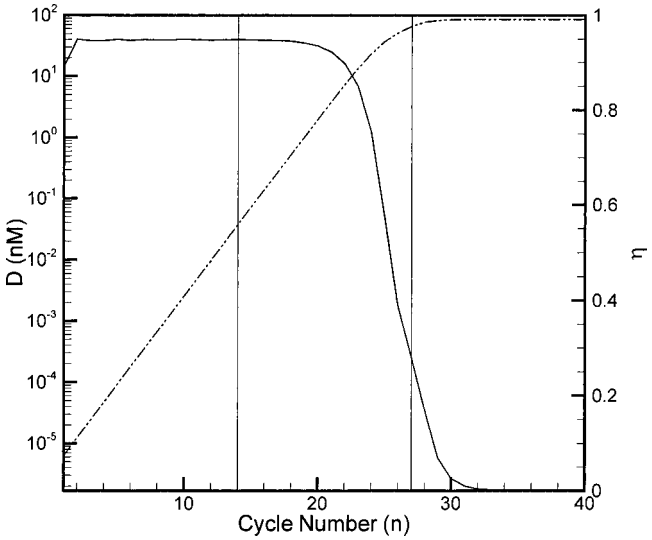

Figure 8. Variation of template concentration and efficiency obtained from simulating a typical real-time PCR experiment. The linear range of detection for SYBR Green dye is also shown by two vertical lines.

tion D, in our simulation) in the region where intensity varies exponentially with the cycle number. The efficiency is then computed from the exponent. Since the first few points are below the detection limit, one may fit the exponential curve only to the data range that is above the detection threshold ($13 < n < 25$). Using that approach, η_{eff} was estimated to be 0.90.

The estimated values of $D_{(0)}$ for the above methods are listed in Table IVa along with the value obtained using $\eta_{\text{eff}} = 1$. For ideal efficiency, the initial concentration is underestimated by 48%. The exponential fit using data in the detection limit grossly overestimates $D_{(0)}$. The standard curve method is found to be most accurate in this case. Note the exponential curve method is highly sensitive to the number of points used in estimating the efficiency. For $19 < n < 25$, $\eta_{\text{eff}} = 0.83$ and the estimate for $D_{(0)}$ exceeds by 272%.

$D_{(0)}$ is inversely proportional to the C_T power of η_{eff}. As a result, a small error in estimation of η_{eff} leads to a large error in prediction of $D_{(0)}$ (see Table IVa and Table IVb). η_{eff} is introduced to approximate $\prod_{i=1}^{C_T}(1+\eta_i)$ by $(1+\eta_{\text{eff}})^{C_T}$. If η_i is constant, all methods give η_{eff} equal to η_i, and $D_{(0)}$ is obtained accurately. Deviations of η_i from a constant value introduce error in the estimation of $D_{(0)}$. This is evident in the exponential fit method using data in the detection range,

Table IVa. Comparison of methods to calculate efficiency.

Analysis method	η_{eff}	$D_{(0)}$ (nM)	$D_{(0)}/D_{(0),\text{exact}}$
Ideal efficiency	1	1.73×10^{-6}	0.52
Standard curve	0.95	3.23×10^{-6}	0.97
Exponential fit–Detection limit ($13 < n < 25$)	0.90	5.25×10^{-6}	1.58
Exponential Fit–Detection Limit ($19 < n < 25$)	0.83	1.24×10^{-6}	3.72

Table IVb. Comparison of methods to calculate efficiency, in the presence of primer dimmers.

Analysis method	η_{eff}	$D_{(0)}$ (nM)	$D_{(0)}/D_{(0),\text{exact}}$
Ideal efficiency	1	6.45×10^{-7}	0.23
Standard curve	0.84	5.75×10^{-6}	1.59
Exponential fit–Detection limit ($13 < n < 25$)	0.82	6.94×10^{-6}	2.05
Exponential fit–Detection limit ($19 < n < 25$)	0.75	1.71×10^{-6}	5.04

where η_i deviates from its constant value of 0.95 over a significant number of data points used.

Formation of primer dimers that undergo extension reactions can affect the calculation of reaction efficiency. Table IVb lists the η_{eff} and $D_{(0)}$ obtained by different methods in a simulation that includes primer dimerization. The performance of the standard curve method is significantly deteriorated. The error in the exponential curve fit method in the detection limit also increases from 58% to 105%. The values listed in Table IVa and Table IVb correspond to a primer concentration of 0.2 μM. Similar trends are observed for higher primer concentrations of 1 and 2 μM. Note that the contribution of primer dimers to the total fluorescence intensity is not considered here. With increasing primer concentration, the concentration of primer dimers also increases, and therefore could have a significant contribution to the total fluorescence.

Real-time PCR is used as a high throughput technique to quantify a large number of genes simultaneously. It is best to operate in the constant efficiency regime so as to reduce error in $D_{(0)}$ estimation. To achieve constant efficiency for all the genes, one approach is to have primer in excess. However, this can lead to primer dimerization and may not be suitable for chemistries where primer dimers contribute to the overall fluorescence. An alternative approach may be to work under nucleotide limiting conditions where efficiency remains constant followed by a steep drop that can be detected by decreasing target DNA concentration.

CONCLUSIONS

We have developed a comprehensive kinetic model for PCR. A large number of interplaying factors affect the performance of PCR. During the course of the reaction, the concentration ratios of the different species vary over many orders of magnitude. This results in a large variation in the rate of competing reactions and changes the relative contribution of those competing reactions to the amplification of template DNA. The model allows us to systematically investigate the effect of different reactant concentrations on template amplification rate. The amplification efficiency is found to be constant initially followed by a gradual decrease when primer concentration becomes rate limiting. In contrast, the amplification efficiency drops steeply in nucleotide limiting conditions. Our analysis also reveal an inverse dependence of template amplification on the primer concentration under

the condition of enzyme concentration being rate limiting. For perfect efficiency, all single strands should be converted to single stranded–primer complexes in each round of reannealing. We show that in order to achieve this, a high ratio of primer to substrate needs to be maintained along with a high primer concentration. The present work reveals new insights into the complex PCR process, especially the conditions that may increase the accuracy of initial template concentration estimation. We hope the model will facilitate the analysis of PCR and these new insights will lead to a better design of assays.

NOMENCLATURE

D	Double-stranded DNA template (to be amplified)
D_i	Incomplete double-stranded DNA with i nucleotides added to the SP complex
D_{inc}	Sum of all incomplete DNA molecules
$D_{(i)}$	Concentration of D at the end of ith cycle
S	Single-stranded template sense
S'	Single-stranded template anti-sense
P	Sense primer
P'	Anti-sense primer
SP	Single-stranded template-primer complex
$E \cdot SP$	Single-stranded template-primer-enzyme complex
R	Primer dimer
N	Nucleotide A,T,G,C
L	Length of target DNA to be amplified
L_P	Length of sense primer
E_0	Total enzyme (Taq polymerase)
E	Active enzyme (DNA polymerase) in solution
E_i	Inactivated enzyme
$F_{(i)}$	Fluorescence at cycle i
η	Cycle efficiency
η_{eff}	Effective efficiency
t_{melt}	Melting cycle time
t_{anneal}	Annealing cycle time
t_{extn}	Extension cycle time

APPENDIX

For a processive enzyme, the reaction equations for the addition of nucleotide to the substrate–primer complex are as follows:

$$E + SP \underset{k_{-e}}{\overset{k_e}{\longleftrightarrow}} E \cdot SP$$

$$E \cdot SP + N \underset{k_{-n}}{\overset{k_n}{\longleftrightarrow}} (E \cdot SP \cdot N) \xrightarrow{k_{cat}} E \cdot D_1$$

$$E \cdot D_1 + N \underset{k_{-n}}{\overset{k_n}{\longleftrightarrow}} (E \cdot D_1 \cdot N) \xrightarrow{k_{cat}} E \cdot D_2$$

$$\vdots$$

$$E \cdot D_{n-1} + N \underset{k_{-n}}{\overset{k_n}{\longleftrightarrow}} (E \cdot D_{n-1} \cdot N) \xrightarrow{k_{cat}} E \cdot D_n$$

$$E \cdot D_n \xrightarrow{k_{cat}} E + D$$

$$\sum_{i=1}^{n-1} D_i = D_{inc}$$

The rate of change of each of the intermediates can therefore be written as:

$$\frac{d[D_n]}{dt} = k'_{\text{cat}}[E \cdot D_n]$$

$$\frac{d[E \cdot D_n]}{dt} = k_{\text{cat}}[E \cdot D_{n-1} \cdot N] - k'_{\text{cat}}[E \cdot D_n]$$

$$\frac{d[E \cdot D_{n-1}]}{dt} = k_{\text{cat}}[E \cdot D_{n-2} \cdot N] - k_n[E \cdot D_{n-1}][N] + k_{-n}[E \cdot D_{n-1} \cdot N]$$

$$\vdots$$

$$\frac{d[E \cdot D_1]}{dt} = k_{\text{cat}}[E \cdot SP \cdot N] - k_n[E \cdot D_1][N] + k_{-n}[E \cdot D_1 \cdot N]$$

$$\frac{d[E \cdot SP]}{dt} = k_e[E][SP] - k_{-e}[E \cdot SP] - k_n[E \cdot SP][N] + k_{-n}[E \cdot SP \cdot N]$$

$$\frac{d[E \cdot SP \cdot N]}{dt} = k_n[E \cdot SP][N] - (k_{-n} + k_{\text{cat}})[E \cdot SP \cdot N]$$

$$\vdots$$

$$\frac{d[E \cdot D_{n-1} \cdot N]}{dt} = k_n[E \cdot D_{n-1}][N] - (k_{-n} + k_{\text{cat}})[E \cdot D_{n-1} \cdot N]$$

Assuming, pseudo-steady state for the intermediates where $[E \cdot D_{n-1} \cdot N]$ where $T = SP, D_1, \ldots, D_{n-1}$, one can derive the following relations:

$$[E \cdot T \cdot N] = \frac{k_n[E \cdot T][N]}{k_{-n} + k_{cat}} = \frac{[E \cdot T][N]}{K_N}$$

$$k_n[E \cdot T][N] - k_{-n}[E \cdot T \cdot N] = k_{cat}[E \cdot T \cdot N]$$

where, $K_N = \frac{(k_{-n} + k_{\text{cat}})}{k_n}$,
The total enzyme concentration E_0 is then equal to,

$$E_0 = E + \sum_{T=SP}^{T=D_{n-1}} (E \cdot T + E \cdot T \cdot N) + E \cdot D_n$$

Substituting $[E \cdot T \cdot N]$ and simplifying for free-enzyme concentration E gives,

$$E = [E_0] - [E \cdot D_n] - \frac{K_N + [N]}{K_N} \left(\sum_{T=SP}^{D_{n-1}} [E \cdot T] \right)$$

Therefore,

$$\frac{\mathrm{d}[D_n]}{\mathrm{d}t} = k'_{\mathrm{cat}}[E \cdot D_n]$$

$$\frac{\mathrm{d}[E \cdot D_n]}{\mathrm{d}t} = k_{\mathrm{cat}} \frac{[E \cdot D_{n-1}][N]}{K_N} - k'_{\mathrm{cat}}[E \cdot D_n]$$

$$\frac{\mathrm{d}[E \cdot T]}{\mathrm{d}t} = k_{\mathrm{cat}} \frac{[E \cdot T_{i-1}][N]}{K_N} - k_{\mathrm{cat}} \frac{[E \cdot T][N]}{K_N}$$

$$\frac{\mathrm{d}[E \cdot SP]}{\mathrm{d}t} = k_e[E][SP] - k_{-e}[E \cdot SP] - k_{\mathrm{cat}} \frac{[E \cdot SP][N]}{K_N}$$

$$\frac{\mathrm{d}[SP]}{\mathrm{d}t} = k_{-e}[E \cdot SP] - k_e[E][SP]$$

$$\frac{\mathrm{d}[N]}{\mathrm{d}t} = \frac{k_{\mathrm{cat}}[N]\left(\sum_{T=SP}^{D_{n-1}} [E \cdot T]\right)}{K_N}$$

References

Anderson MLM, Young BD. 1985. Quantitative filter hybridization. In: Hames BD, Higgins SJ, editors. Nucleic acid hybridization: A practical approach. Oxford and Washington, DC: IRL Press. pp 73–111.

Breslauer KJ, Bina-Stein M. 1977. Relaxation kinetics of the helix-coil transition of a self-complementary ribo-oligonucleotide: A7U7. Biophys Chem 7(3):211–216.

Bustin SA. 2000. Absolute quantification of mRNA using real-time reverse transcription polymerase chain reaction assays. J Mol Endocrinol 25(2): 169–193.

Craig ME, Crothers DM, Doty P. 1971. Relaxation kinetics of dimer formation by self complementary oligonucleotides. J Mol Biol 62(2): 383–401.

Datta K, LiCata VJ. 2003. Thermodynamics of the binding of Thermus aquaticus DNA polymerase to primed-template DNA. Nucleic Acids Res 31(19):5590–5597.

Einolf HJ, Guengerich FP. 2000. Kinetic analysis of nucleotide incorporation by mammalian DNA polymerase delta. J Biol Chem 275(21):16316–16322.

Giulietti A, Overbergh L, Valckx D, Decallonne B, Bouillon R, Mathieu C. 2001. An overview of real-time quantitative PCR: Applications to quantify cytokine gene expression. Methods 25(4):386–401.

Gotoh M, Hasegawa Y, Shinohara Y, Shimizu M, Tosu M. 1995. A new approach to determine the effect of mismatches on kinetic parameters in DNA hybridization using an optical biosensor. DNA Res 2(6):285–293.

Hsu JT, Das S, Mohapatra S. 1997. Polymerase chain reaction engineering. Biotech Bioeng 55(2):359–366.

Jensen KK, Orum H, Nielsen PE, Norden B. 1997. Kinetics for hybridization of peptide nucleic acids (PNA) with DNA and RNA studied with the BIAcore technique. Biochemistry 36(16):5072–5077.

Jung R, Soondrum K, Neumaier M. 2000. Quantitative PCR. Clin Chem Lab Med 38(9):833–836.

Liu W, Saint DA. 2002a. A new quantitative method of real time reverse transcription polymerase chain reaction assay based on simulation of polymerase chain reaction kinetics. Anal Biochem 302(1):52–59.

Liu W, Saint DA. 2002b. Validation of a quantitative method for real time PCR kinetics. Biochem Biophys Res Commun 294(2):347–353.

Lowe LG, Guengerich FP. 1996. Steady-state and pre-steady-state kinetic analysis of dNTP insertion opposite 8-oxo-7,8-dihydroguanine by *Escherichia coli* polymerases I exo- and II exo. Biochemistry 35(30): 9840–9849.

Mathieu-Daude F, Welsh J, Vogt T, McClelland M, Hiltunen T, Raja-Honkala M, Nikkari T, Yla-Herttuala S, Hwang IT, Kim YJ, Kim SH, Kwak CI, Gu YY, Chun JY, Czerny T. 1996. DNA rehybridization during PCR: The 'Cot effect' and its consequences. Nucleic Acids Res 24(11):2080–2086.

Ponchel F, Toomes C, Bransfield K, Leong FT, Douglas SH, Field SL, Bell SM, Combaret V, Puisieux A, Mighell AJ, Robinson PA, Inglehearn CF, Isaacs JD, Markham AF. 2003. Real-time PCR based on SYBR-Green I fluorescence: An alternative to the TaqMan assay for a relative quantification of gene rearrangements, gene amplifications and micro gene deletions. BMC Biotechnol 3(1):18.

Qiagen. 2002a. QuantiTect SYBR Green PCR Handbook.

Qiagen. 2002b. Taq PCR handbook.

Record MT. 1972. Kinetics of the helix-coil transition in DNA. Biopolymers 11(7):1435–1484.

Rengarajan K, Cristol SM, Mehta M, Nickerson JM. 2002. Quantifying DNA concentrations using fluorometry: A comparison of fluorophores. Mol Vis 8:416–421.

Schnell S, Mendoza C. 1997a. Enzymological considerations for a theoretical description of the quantitative competitive polymerase chain reaction (QC-PCR). J Theor Biol 184(4):433–440.

Schnell S, Mendoza C. 1997b. Theoretical description of the polymerase chain reaction. J Theor Biol 188(3):313–318.

Stolovitzky G, Cecchi G. 1996. Efficiency of DNA replication in the polymerase chain reaction. Proc Natl Acad Sci USA 93(23):12947–12952.

Tosaka A, Ogawa M, Yoshida S, Suzuki M. 2001. O-helix mutant T664P of Thermus aquaticus DNA polymerase I: Altered catalytic properties for incorporation of incorrect nucleotides but not correct nucleotides. J Biol Chem 276(29):27562–27567.

Velikanov MV, Kapral R. 1999. Polymerase chain reaction: A Markov process approach. J Theor Biol 201(4):239–249.

Wartell RM, Benight AS. 1985. Thermal denaturation of DNA molecules: A comparision of theory with experiment. Phys Reports (Review Section of Physics Letters) 126(2):67–107.

Wetmur JG, Davidson N. 1968. Kinetics of renaturation of DNA. J Mol Biol 31(3):349–370.

Wittwer CT, Herrmann MG, Moss AA, Rasmussen RP. 1997. Continuous fluorescence monitoring of rapid cycle DNA amplification. Biotechniques 22(1):130–131, 134–138.

Yuen T, Wurmbach E, Pfeffer RL, Ebersole BJ, Sealfon SC. 2002. Accuracy and calibration of commercial oligonucleotide and custom cDNA microarrays. Nucleic Acids Res 30(10):e48